Am J Physiol Regul Integr Comp Physiol 299: R140–R149, 2010.
First published April 21, 2010; doi:10.1152/ajpregu.00535.2009.

Central melanocortin stimulation increases phosphorylated perilipin A and hormone-sensitive lipase in adipose tissues

Y. B. Shrestha,[1] C. H. Vaughan,[1,2] B. J. Smith, Jr.,[1] C. K. Song,[1,2] D. J. Baro,[1] and T. J. Bartness[1,2]

[1]*Department of Biology, and* [2]*Center for Behavioral Neuroscience, Georgia State University, Atlanta, Georgia*

Submitted 26 August 2009; accepted in final form 19 April 2010

Shrestha YB, Vaughan CH, Smith BJ Jr, Song CK, Baro DJ, Bartness TJ. Central melanocortin stimulation increases phosphorylated perilipin A and hormone-sensitive lipase in adipose tissues. *Am J Physiol Regul Integr Comp Physiol* 299: R140–R149, 2010. First published April 21, 2010; doi:10.1152/ajpregu.00535.2009.—Norepinephrine (NE) released from the sympathetic nerves innervating white adipose tissue (WAT) is the principal initiator of lipolysis in mammals. Central WAT sympathetic outflow neurons express melanocortin 4-receptor (MC4-R) mRNA. Single central injection of melanotan II (MTII; MC3/4-R agonist) nonuniformly increases WAT NE turnover (NETO), increases interscapular brown adipose tissue (IBAT) NETO, and increases the circulating lipolytic products glycerol and free fatty acid. The WAT pads that contributed to this lipolysis were inferred from the increases in NETO. Because phosphorylation of perilipin A (p-perilipin A) and hormone-sensitive lipase are necessary for NE-triggered lipolysis, we tested whether MTII would increase these intracellular markers of lipolysis. Male Siberian hamsters received a single 3rd ventricular injection of MTII or saline. Trunk blood was collected at 0.5, 1.0, and 2.0 h postinjection from excised inguinal, retroperitoneal, and epididymal WAT (IWAT, RWAT, and EWAT, respectively) and IBAT pads. MTII increased circulating glycerol concentrations at 0.5 and 1.0 h, whereas free fatty acid concentrations were increased at 1.0 and 2.0 h. Western blot analysis showed that MTII specifically increased p-perilipin A and hormone-sensitive lipase only in fat pads that previously had MTII-induced increases in NETO. Phosphorylation increased in IWAT at all time points and IBAT at 0.5 h, but not RWAT or EWAT at any time point. These results show for the first time in rodents that p-perilipin A can serve as an in vivo, fat pad-specific indictor of lipolysis and extend our previous findings showing that central melanocortin stimulation increases WAT lipolysis.

sympathetic nervous system; method; Western blot analysis

WHEN ENERGY NEEDS CANNOT BE met by circulating fuels or stored carbohydrates, lipid stored primarily as triacylglycerol in adipocytes is mobilized through the process of lipolysis (43). Increased sympathetic nervous system (SNS) drive to white adipose tissue (WAT) is the principal initiator of lipolysis in mammalian adipocytes (for reviews see Refs. 6 and 8). The hydrolysis of triacylglycerol to glycerol and free fatty acids (FFA) begins with the binding of norepinephrine (NE), the primary postganglionic sympathetic neurotransmitter, to β-adrenoceptors located on adipocyte membranes (for a review see Ref. 35).

We first described the central nervous system origins of the SNS outflow from brain to WAT using viral transneuronal tract-tracing methodology employing pseudorabies virus (4). These data did not suggest the central neurochemicals involved in the control of the sympathetic drive to WAT. Melanocortins are one possible neurochemical. For example, central melanocortin receptor stimulation via intraventricular administration of melanotan II (MTII), a synthetic analog of the natural agonist of the melanocortin 3- and 4-receptors (MC3/4-R), α-melanocyte stimulating hormone, triggers decreases in body fat of laboratory rats greater than can be accounted for by its ability to inhibit food intake (47). That this effect likely is caused by MC4-R activation, even though MTII binds to both MC3- and MC4-Rs, is based on the overwhelming evidence suggesting the primacy of MC4-Rs in energy balance (49). This led us to test whether the SNS outflow circuitry from brain to WAT contained neurons that expressed MC4-R mRNA (52), and we conducted an analogous test for brown adipose tissue [BAT; (53)] as well. MC4-R mRNA was extensively colocalized on these sympathetic outflow neurons (~60% of all pseudorabies virus-labeled neurons for both tissues across the neuroaxis) demonstrated by combining pseudorabies virus immunohistochemical labeling of the SNS outflow to WAT and to BAT with in situ hybridization for MC4-R mRNA (52, 53). Moreover, and functionally, a single 3rd ventricular (3V) injection of MTII triggered differential sympathetic drive across WAT depots and interscapular BAT [IBAT; (14)]. Specifically, NE turnover (NETO) was increased in IWAT and dorsosubcutaneous WAT (DWAT), and also in IBAT, but not epididymal or retroperitoneal WAT [EWAT and RWAT, respectively (14)]. In addition, this central MTII administration significantly provoked increases in the circulating lipolytic products glycerol and FFA (14), as well as triggering increases in IBAT temperature (thermogenesis) (14). We found that other lipolytic stimuli, such as glucoprivation (2-deoxy-D-glucose treatment), cold exposure, and food deprivation, each produced unique patterns of differential sympathetic drive (NETO) across fat pads (signature SNS drive patterns) and significantly triggered increases in circulating glycerol and FFAs (15). Although it is assumed that WAT pads with increases in NETO would be the principal contributors to the increases in circulating FFA and glycerol, this might not necessarily be the case. For example, even though the vast majority of triacylglycerol is stored in WAT pads, other tissues, such as liver, and to lesser degrees, muscle and BAT, also store triacylglycerol and could potentially contribute to increases in the circulating concentrations of these products of lipolysis in addition to other WAT pads we did not assay. Thus, there is a need for an in vivo indicator of catecholamine-stimulated lipolytic activity that would indicate lipid mobilization on a fat pad-specific basis.

Phosphorylation of hormone-sensitive lipase (p-HSL) and perilipin A (p-perilipin A) were selected as potential intracellular markers of catecholamine-stimulated lipolysis due to their critical role in triacylglycerol hydrolysis. Specifically, catecholamines induce lipolysis in adipocytes after binding to

Address for reprint requests and other correspondence: T. J. Bartness, Dept. of Biology, Georgia State Univ., 24 Peachtree Center Ave. NE, Atlanta, Georgia 30302-4010 (e-mail: bartness@gsu.edu).

adrenoceptors (β_{1-3}) coupled to G proteins (for reviews see Refs. 20 and 33). The β_3-adrenoceptor is the β-adrenoceptor subtype predominantly involved in lipolysis in rodents (38) (for a review see Ref. 2). The β-adrenoceptor-coupled stimulatory G proteins activate adenylate cyclase resulting in increased intracellular cyclic adenosine monophosphate. This, in turn, activates PKA complex leading to p-HSL and p-perilipin A (for a review see Ref. 12). Perilipin A is an intracellular lipid droplet surface-associated protein in adipocytes (29), whereas, HSL is an intracellular triacylglycerol lipase found in adipocytes (for a review see Ref. 32). Phosphorylation of HSL by PKA triggers the translocation of HSL from the cytoplasm to the lipid droplet where it can exert its lipase activity (26). Perilipin A is abundantly localized in adipocyte lipid droplets and functions to increase cellular triacylglycerol storage by decreasing the rate of triacylglycerol hydrolysis (13, 40, 55, 58). Consequently, perilipin A-knockout mice display severely attenuated β-adrenergic-induced lipolysis, suggesting perilipin A is essential for PKA-mediated lipolysis (40, 58). PKA phosphorylation of perilipin A provides HSL access to the lipid droplet through varied and debated mechanisms (for reviews see Refs. 2 and 17).

In addition to HSL, another important lipase in adipocytes is adipose triglyceride lipase. Adipose triglyceride lipase predominantly is involved in basal lipolysis (36, 48) and appears to be required for all PKA-stimulated FFA release in the absence of HSL. Although adipose triglyceride lipase seems important for cAMP-dependent PKA stimulation of FFA release, without the activation of HSL and perilipin A, complete lipolysis of triacylglycerol to its hydrolytic end products of glycerol and FFA cannot be achieved (27).

In addition to their critical role in NE-induced lipolysis, PKA-induced p-perilipin A and p-HSL also is necessary for the complete expression of SNS/NE-stimulated BAT thermogenesis (54). Therefore, it seems that levels of p-perilipin A and p-HSL could serve as fat pad-specific in vivo indicators of catecholamine-induced lipolysis and BAT thermogenesis. As a test of this hypothesis, we chose the stimulation of central melanocortin receptors by MTII that we previously have shown increases NETO to some WAT pads and to IBAT (14), as discussed above. This was accomplished by giving a single injection of MTII or the saline vehicle into the 3V of male Siberian hamsters. Subsequently, we conducted Western blot analysis on homogenates of IWAT, EWAT, RWAT, and IBAT to measure p-perilipin A and p-HSL. We also measured circulating concentrations of the lipolytic products glycerol and FFA as more global measures of lipid mobilization. The results of this experiment represent the first study to show that p-perilipin A can effectively be used as fat pad-specific lipolytic indicator in vivo in rodents, in this case marking central melanocortin receptor agonism-induced lipolysis by IWAT and IBAT, but not EWAT or RWAT.

MATERIALS AND METHODS

Animals and handling. Eighty male Siberian hamsters weighing between 35 and 50 g were obtained from our breeding colony. The hamsters were single housed in plastic cages (23×26×30 cm) and provided with food (Rodent Chow 5001; Purina, St. Louis, MO) and tap water ad libitum. The animals were housed at room temperature (23°C) in a long-day photoperiod (16:8-h light-dark, lights on at 0300 h). Guide cannulae targeted for the 3V were stereotaxically implanted into the hamsters 1 wk after single housing (see *3V cannula implantation and injection protocol*). Two weeks postcannulation, hamsters were divided into two groups matched on both body mass and the percent change in body mass between single housing and recovery from cannulation surgery. It is critical to emphasize that handling and injection each or together can increase sympathetic drive to WAT or BAT (unpublished observations), thus potentially obfuscating an effect of the lipolytic stimulus on NETO, in this case central melanocortin receptor agonism. Therefore, each hamster was weighed and handled every day for 5 min for 3 wk to adapt them to the handling associated with the injection procedure and thereby minimize stress-induced increases in sympathetic drive. Housing and all procedures were approved by the Georgia State University Institutional Animals Care and Use Committee and were in accordance with the Public Health Service and U.S. Department of Agriculture guidelines.

3V cannula implantation and injection protocol. Procedures for 3V cannulae implantation and injections were performed as described similar to our previous reports (14, 21). In brief, a guide cannula (26-gauge stainless steel; Plastics One, Roanoke, VA) was implanted (level skull; anterior-lateral from bregma, 0 mm; medial-lateral from midsaggital sinus, 0 mm; and dorsal-ventral, −5.5 mm from the top of the skull) targeted for placement just above the 3V. The cannulae were secured to the skull using cyanoacrylate ester gel, two 3/16-mm jeweler's screws, and dental acrylic. A removable obturator (Plastics One) sealed the opening in the guide cannula throughout the experiment, except when it was removed for the injections. Hamsters were injected into the 3V with saline (200 nl) for three consecutive days before the test day to further acclimatize the hamsters to the injection procedure. On the test day at 0600 h, hamsters were transferred from the housing facility to the test room, food was removed from their cheek pouches, food hopper, and bedding, and they were given continued access to water. A 3-h delay in the injection was installed to help equalize the time since food was last eaten across the animals, because Siberian hamsters eat approximately every 3 to 4 h (7), but was not long enough to produce a substantial period of food deprivation. In addition, this period served to calm the animals from any stress associated with weighing and the depouching of food. At the end of this period, hamsters received a single injection of either the sterile saline vehicle or MTII (5 nmol; 200 nl each). We chose the 5-nmol MTII dose because we previously found it to be the most effective dose in inducing increases in circulating glycerol and FFA concentrations (but not circulating NE or epinephrine) and in increasing NETO to IWAT and DWAT as well as IBAT in Siberian hamsters (14).

Terminal measures and 3V cannulae placement verification. Following the single injection of MTII or saline, hamsters were decapitated 0.5, 1.0, or 2.0 h postinjection. Trunk blood was collected and stored on ice. IBAT, IWAT, EWAT, and RWAT were excised from both sides, immediately minced on dry ice, snap frozen in liquid nitrogen, and stored at −80°C until analysis. Immediately after decapitation, 200 nl of toluidine blue was injected into the cannulae to help confirm placement of the cannula in the 3V. The brains were removed and then sliced manually using the optic chiasm as a landmark to verify cannula placement. Only data from animals with dye visible in any portion of the 3V were analyzed.

Plasma FFA and glycerol measurement. Trunk blood was kept at 4°C overnight and then centrifuged for 20 min (3,000 rpm at 4°C). Serum was removed and stored at −80°C until assayed. Serum FFAs (HR Series NEFA-HR; Wako Pure Chemical Industries, Osaka, Japan) and serum glycerol (Free Glycerol Reagent; Sigma-Aldrich, St Louis, MO) were measured according to the manufacturers' directions.

Western blot assay. The frozen adipose tissues were homogenized using handheld glass homogenizers (Dounce homogenizer) in lipid-associated protein extraction buffer modified from Greenberg et al. (29) containing 50 mM HEPES, 100 mM NaCl, 10% SDS, 2 mM EDTA, 0.5 mM DTT, 1 mM benzamidine, and protease inhibitor

cocktail (Calbiochem, EMD Chemicals, Gibbstown, NJ) at 50 μl/g of tissue and phosphatase inhibitor cocktail (Halt; Pierce, Thermo Fischer Scientific, Rockford, IL) as per the manufacturer's recommendations. Homogenates were incubated at 37°C with constant agitation and vigorously vortexed every 5 min during the 1-h incubation. The homogenates were then centrifuged at 13,000 rpm for 10 min at room temperature and the infranatant was carefully removed and recentrifuged. Subsequently, the infranatant containing the protein extract was aliquoted and stored at −80°C. An aliquot from each tissue extract was used to determine protein content using the bicinchoninic acid protein assay kit (Thermo Fisher Scientific). Samples of the tissue containing 10 μg of protein were mixed with loading buffer at 2× final concentration and heated at 95°C for 5 min, electrophoresed on a low-bis SDS-PAGE [10%:0.07% acrylamide:bis (29)] and transferred to polyvinylidene difluoride membranes. One membrane representing a single gel was cut to separate duplicate lanes so that the duplicate lanes could be probed independently with different antibodies. Cut membranes were blocked with 4% nonfat dry milk in Tris-buffered saline for 2 h at room temperature, and duplicate lanes were separately incubated with different primary antibodies at 4°C overnight in the same buffer [anti-perilipin A affinity purified antibody (Sigma Aldrich), anti-phospho-(Ser/Thr) PKA substrate antibody (Cell Signaling Technology, Danvers, MA), anti-phospho-HSL (Ser660) antibody and anti-HSL antibody (Cell Signaling Technology)]. Immunoblots were rinsed in Tris-Tween 20 buffered saline (TTBS) for 5 min (4×) and incubated with goat anti-rabbit alkaline phosphatase (AP)-conjugated secondary antibody (Immun-Star AP Chemiluminescent Kits; Bio-Rad Laboratories, Hercules, CA) at room temperature for 2 h. Finally, the membranes were washed in TTBS for 10 min (3×), duplicate lanes from a single gel were reassembled side by side onto a solid support and incubated with Immun-Star AP substrate. The chemiluminescent bands were visualized using an Innotech Bioimager (Alpha Innotech, San Leandro, CA), and their band intensities were quantified using the associated densitometric software as described in Baro et al. (5). Regarding all immunoblot figures presented herein; backgrounds were minimized by adjusting the brightness/contrast using Adobe Photoshop. In addition, images were cropped to the area of interest (for example, 62–67 kDa smear for perilipin A) using Adobe Photoshop, as this was the only area quantified. It should be noted that the anti-phosphorylated-PKA (anti-p-PKA) recognized several bands outside of this region. Note that the figures are presented as a composite of the duplicate samples probed with different antibodies.

Antibody characterization. Anti-p-(Ser/Thr) PKA substrate antibody was raised in rabbits with a synthetic p-PKA substrate peptide (KLH-coupled) and does not cross-react with the non-p-PKA substrate motif, but cross-reacts to endogenous p-PKA substrate motif of all species as per the manufacturer's product description. Anti-perilipin A antibody was developed in rabbit using synthetic peptide corresponding to amino acid residues 492–505 of human perilipin A (KLH-coupled) with the corresponding sequence differing by one residue in mouse and rat, and affinity purified using the immunizing peptide immobilized on agarose as noted in the manufacturer's product description. Anti-p-HSL (Ser660) antibody was produced in rabbits with synthetic phospho-peptide (KLH-coupled) corresponding to residues surrounding Ser651 of mouse HSL (equivalent to Ser660 of rat HSL) and is cross-reactive to rats and mice according to the manufacturer's product description. Anti-HSL antibody was raised in rabbits with a synthetic peptide derived from the sequence of human HSL and is cross-reactive to humans and rats according to the manufacturer's product description.

Immunoprecipitation of perilipin A for verification of perilipin A. Male hamsters were injected with MTII (5 nmol) or saline into the 3V, and 2 h later, both IWAT pads were excised, minced, and snap frozen in liquid nitrogen. A 300-mg IWAT sample from each animal was homogenized and processed as described above. Total perilipin A in a 100-μl homogenate infranatant was immunoprecipitated (IPG kit; Sigma-Aldrich) using the perilipin A antibody raised in guinea pig (Fitzgerald Industries, Concord, MA). The immunoprecipitated perilipin A samples were run in duplicates on SDS-PAGE low-bis gel [10%:0.07% acrylamide/bis (29)], and separate lanes from the immunoblot were probed separately with p-PKA substrate or perilipin A antibodies (Fig. 1). Therefore, Fig. 1 is a composite of duplicate samples probed with the different antibodies.

Dephosphorylation of perilipin A with protein phosphatase 1 for verification of p-perilipin A. It is established that perilipin A is major substrate for PKA and contains six PKA phosphorylation sites (29, 30, 57). Because a specific antibody to detect p-perilipin A is not available, an alternate method using the anti-p-PKA substrate antibody to detect p-perilipin A is widely used (e.g., Refs. 19, 39, and 41). It has been demonstrated that dephosphorylation of perilipin A is predominantly carried out by protein phosphatase 1 (PP1) in adipocytes (18). To confirm that the signal detected with PKA substrate in the immunoprecipitated sample was p-perilipin A, we treated the adipocyte homogenate with PP1 as per the manufacturer's recommendation (New England Biolabs, Ipswich, MA) before immunoprecipitation to remove phosphate groups from p-perilipin A. This should result in reduced p-PKA substrate signal on a Western blot analysis compared with nontreated homogenates. The ratio of p-perilipin A to total perilipin A was markedly reduced in PP1-treated samples compared with the control group (Fig. 1). This unequivocally demonstrates that the bands detected with anti-p-PKA substrate antibody in the immunoprecipitated perilipin A samples were actually p-perilipin A.

Statistical analysis. Data from saline- and MTII-treated hamsters were analyzed using the Sigma Plot statistical software (version 11.0; Systat Software San Jose, CA). Student's *t*-tests were performed between saline and MTII-treated groups within the same time periods of 0.5, 1.0, and 2.0 h, respectively. Means between the saline and MTII groups were considered significant if $P < 0.05$. Exact probabilities and test values have been omitted for simplification and clarity of the presentation of the results.

RESULTS

Central injections of MTII alter the phosphorylation state of WAT perilipin A. We measured in vivo changes in phosphorylation of perilipin A in response to central injection of MTII (Fig. 1). Perilipin A was first immunoprecipitated from WAT protein extracts of experimental (MTII-treated) and control (saline-treated) animals. Total and PKA-p-perilipin A were then detected in immunoblot assays using antibodies that recognized perilipin A (anti-perilipin A) and p-PKA consensus sequences (anti-p-PKA), respectively (Fig. 1*A*). PKA-p-perilipin A was quantified by dividing the optical density for the signal produced from anti-p-PKA, by the optical density for total perilipin A (signal from anti-perilipin A) (Fig. 1*B*). This ratio metric measure normalized for variations in the perilipin A content in each fat pad mass. A similar protocol has been extensively used to measure changes in p-perilipin A in vitro (e.g., Refs. 19, 42, and 62).

The data shown in Fig. 1 make several important points. First, using our protocol, perilipin A is detected as a 62–67 kDa smear, consistent with its known molecular weight (29). Second, because we have specifically immunoprecipitated perilipin A, the smear detected at 62–67 kDA with anti-p-PKA is unequivocally perilipin A. Third, PP1 treatment markedly reduced the p-perilipin A signal on the immunoblot (Fig. 1, *C–E*). Normalizing the anti-p-PKA signal by the anti-perilipin A signal shows that p-perilipin A was reduced relative to total perilipin A in the PP1-treated samples from MTII-injected, but

A

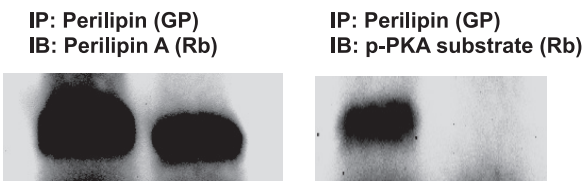

B

	MTII		saline	
	pPKA (OD)	Peri A (OD)	ratio (pPKA/ Peri A)	% of saline
MTII	35635	22495	1.6	311.5
saline	23200	45623	0.5	100.0

C

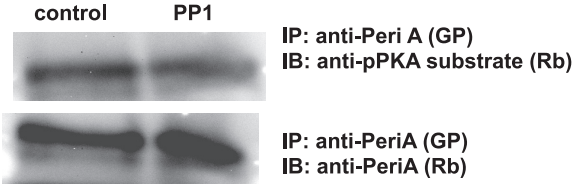

D

	pPKA (OD)	PeriA (OD)	Ratio (pPKA/ PeriA)	% of control
control	3865	6972	0.55	100.0
PP1	3160	9227	0.34	61.8

E

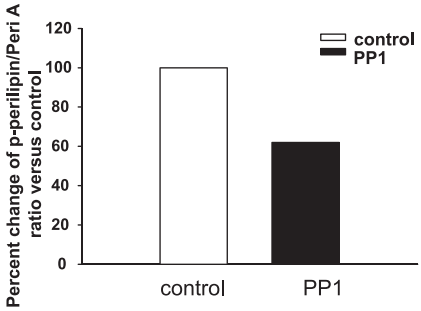

Fig. 1. *A*: perilipin A (Peri A) was immunoprecipitated (IP) from inguinal white adipose tissue (IWAT) homogenates and was run on SDS-PAGE gel. Lanes from the same immunoblot (IB) containing the same preparation were probed separately with anti-phosphorylated-PKA (anti-p-PKA) substrate or anti-Peri A antibodies. IP Peri A was consistently detected at 62–67 kDa with p-PKA substrate and Peri A antibodies, validating that the bands represent Peri A and are phosphorylated by PKA. GP, antibody raised in guinea pig; Rb, antibodies raised in rabbits; MTII, melanotan II. *B*: optical densities (OD) of bands detected with anti-p-PKA substrate and anti-Peri A antibodies and the ratios of p-Peri A over the total Peri A. *C*: IWAT homogenate from an MTII-injected animal that was treated with or without protein phosphatase 1 (PP1), then immunoprecipitated with perilipin antibody (GP) and subsequently immunoblotted separately with PKA substrate or Peri A antibodies. *D*: ODs of bands detected with anti-p-PKA substrate and anti-Peri A antibodies and the ratios of p-Peri A over the total Peri A. *E*: histogram of the ratios of p-Peril A over the total Peri A in the IWAT homogenate of MT II-injected animal, treated either with or without PP1. The ratios are expressed as %change compared with control and the ratio was markedly reduced in PP1-treated samples. Figure 1 is a composite of duplicate samples probed with different antibodies.

not vehicle-injected control animals (Fig. 1, *D* and *E*). Fourth, and most importantly, MTII induced PKA phosphorylation of perilipin A. This can be seen *1*) in Fig. 1*A, left* as a slight increase in the size of the perilipin A smear in WAT samples from the MTII-compared with saline-treated animals, and *2*) in Fig. 1*A, right* by the presence of an anti-p-PKA signal in the WAT protein extracts from the MTII- but not saline-treated animals. Together, the data in Fig. 1 provide compelling evidence that the 62–67 kDa immunoblot signals produced by anti-p-PKA and anti-perilipin A reliably report on p-perilipin A and total perilipin A levels in cell homogenates, respectively. Therefore, in the remainder of the studies reported here, we chose to forego immunoprecipitation of perilipin A. Instead, homogenates in duplicates were directly immunoblotted with anti-p-PKA and anti-perilipin A individually, as has been done in several previously published in vitro studies (e.g., Refs. 19, 42, and 62).

A single 3V MTII injection significantly increased glycerol and FFA circulating concentrations. A single 3V MTII (5 nmol) injection significantly increased the serum glycerol level compared with saline at 0.5 and at 1.0 h postinjection (Fig. 2*A*). MTII also significantly increased serum FFA level at 1.0 and 2.0 h, but not at 0.5 h postinjection (Fig. 2*B*).

A single 3V MTII injection induced significantly increased p-perilipin A and p-HSL in IWAT. A single 3V MTII injection significantly increased the ratio of IWAT p-perilipin A to perilipin A compared with saline at 0.5, 1.0, and at 2.0 h postinjection (Fig. 3*A*). Correspondingly, MTII injection also significantly increased the ratios of IWAT p-HSL to HSL compared with saline at 0.5 and 1.0 h, but not at 2.0 h postinjection (Fig. 3*B*).

A single 3V MTII injection induced significantly increased p-perilipin A and p-HSL in IBAT. A single 3V MTII injection significantly increased the ratio of IBAT p-perilipin A to perilipin A compared with saline at 0.5 h, but not at 1.0 or 2.0 postinjection (Fig. 4*A*). Correspondingly, MTII injection also significantly increased the ratio of IBAT p-HSL to HSL compared with saline at 0.5 h, but not at 1.0 or 2.0 h postinjection (Fig. 4*B*).

A single 3V MTII injection did not induce increased p-perilipin A and p-HSL in RWAT or EWAT. Consistent with a lack of significantly increased NETO in RWAT or EWAT after an identical single 3V MTII injection (14), here MTII did not increase the ratios of p-perilipin A to perilipin A or p-HSL to HSL compared with saline for either RWAT or EWAT at all time points except for a significant increase in RWAT p-HSL to HSL at 2.0 h (Figs. 5 and 6).

DISCUSSION

The results in this study show for the first time that an acute stimulation of central melanocortin receptors significantly increased IWAT and IBAT p-perilipin A and p-HSL, as measured by Western blot analysis, but not in EWAT and RWAT compared with the saline controls. Specifically, the ratios of p-perilipin A to perilipin A induced by a single 3V MTII injection were significantly increased for IWAT at 0.5, 1.0, and 2.0 h postinjection compared with that of the saline controls with corresponding significant increases in the ratios of p-HSL to HSL at 0.5 and 1.0 h, but not at 2.0 h postinjection. Similarly, the ratios of IBAT p-perilipin A to perilipin A and p-HSL to HSL were significantly increased by a single 3V MTII injection compared with that of the saline control, but only at 0.5 h. These increases in WAT p-perilipin A and p-HSL

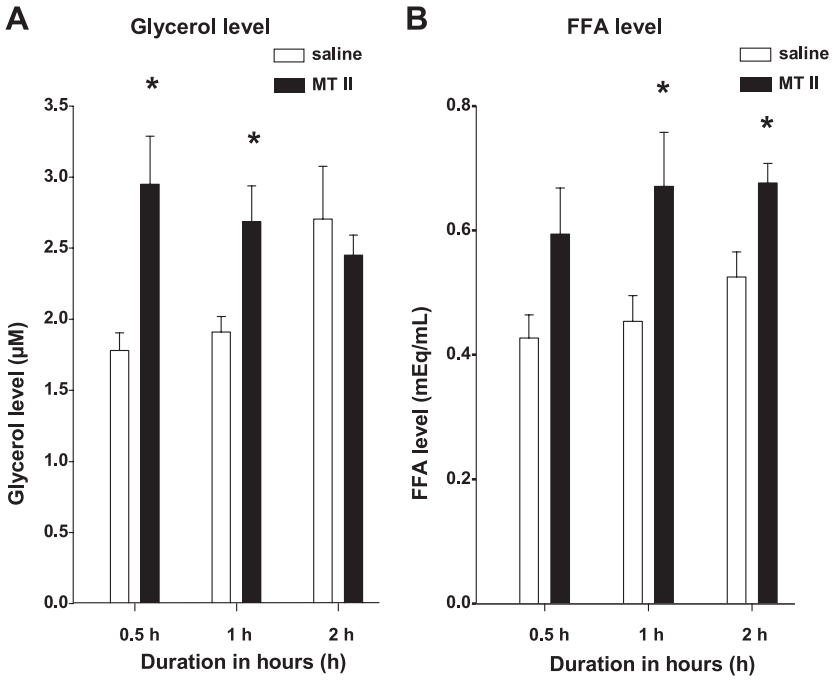

Fig. 2. Mean ± SE serum glycerol (*A*) and free fatty acid (FFA; *B*) concentrations from hamsters injected centrally with MTII 5 nmol (black bars) or saline (white bars) at 0.5, 1, and 2 h later. *$P < 0.05$, MTII vs. saline.

were associated with MTII-induced increased glycerol and FFA plasma concentration, implicating increased WAT lipolysis. These results support our previous findings where identical single 3V MTII injections induced increases in IWAT and IBAT NETO, but not in EWAT and RWAT, a treatment that also provoked significant increases in plasma glycerol and FFA concentrations (14) but did not reveal the exact source of these lipolytic products. Together these findings strongly suggest that the central MTII-induced increases in NETO in IWAT and IBAT (14) resulted in increased lipolysis in these depots as suggested by the increased ratios of p-perilipin A to perilipin A and p-HSL to HSL, proteins known to be involved in catecholamine-induced lipolysis in adipocytes. Thus, it seems likely that IWAT, but not EWAT or RWAT lipolysis, contributed to the increased circulating concentrations of the lipolytic products glycerol and FFAs. Finally, the following three facts strongly suggest that p-perilipin A and p-HSL serve as indicators of SNS-stimulated NE-induced lipolysis in vivo: *1*) lipolysis induced in vitro by catecholamines or more specific β_3-adrenoceptor agonists is dependent on PKA-mediated phosphorylation of perilipin A and HSL, as shown in vitro (1, 37, 56, 58), *2*) the pan-β-adrenoceptor agonist isoproterenol dose-dependently stimulates PKA activity in vitro (25), and *3*) the increased IWAT p-perilipin A and p-HSL reported here in vivo after central melanocortin receptor agonism also significantly increased the sympathetic drive (NETO) to IWAT, but not RWAT or EWAT (14).

We found a significant increase in the ratio of p-HSL to HSL in RWAT at 2.0 h with no change in the ratio of p-perilipin A to perilipin A. Normally the phosphorylation of these two proteins are "lock-stepped" to produce a coordinated lipolytic response (for a review see Refs. 12 and 35). We previously found a strong tendency ($P = 0.06$) for 3V MTII-induced increases in RWAT NETO, suggesting the potential for SNS/NE-induced lipolysis (14). It is puzzling, therefore, that here there was not a corresponding significant or suggestive increase in p-perilipin A. It is possible that this is an example of phosphorylation of HSL independent of PKA. This can occur in Chinese hamster ovary cells where NE activation of the β_3-adrenoceptor coupled to G_i increases the extracellular signal-regulated kinase 1/2-mitogen activated protein kinase pathway (51), leading to increases in HSL activity (1). Whether this can occur in Siberian hamster white adipocytes in vivo is unknown.

Because we used MTII, an MC3/4-R agonist, the effects observed here also could be via MC3-R agonism, although MC4-R is recognized as a more important mediator of melanocortins for changes in energy metabolism (for reviews see Refs. 16 and 49). As with any ventricular application, there is a possibility of leakage into the periphery and thereby a direct effect of MTII on the adipocytes there. White adipocytes do express MC4-R (e.g., Refs. 10 and 31) and α-MSH or MTII stimulate lipolysis (increased FFA release in incubation media) in 3T3L-1 cells in vitro (11). We believe, however, that peripheral leakage seems unlikely to account for the data here, because, as with our previous report of identically applied central MTII, such leakage would not account for the fat pad-specific differential NETO to WAT [i.e., increased IWAT and DWAT NETO, but not RWAT or EWAT (14)] nor for the finding here of a fat pad-specific, differentially increased p-perilipin A and p-HSL (IWAT, but not RWAT and EWAT). Finally, it seems unlikely that the increased IWAT p-perilipin A and p-HSL seen here is due to 3V MTII-induced increased adrenal medullary release of NE and/or epinephrine, because we previously found that identically centrally applied MTII did not increase plasma NE or epinephrine, but as here, plasma glycerol and FFA concentrations were increased compared with saline control injections (14). These results and those of others (e.g., Ref. 45), suggest that central melanocortin receptor agonism triggers WAT lipolysis, likely via stimulation of MC4-R mRNA located on the SNS outflow neurons innervating WAT.

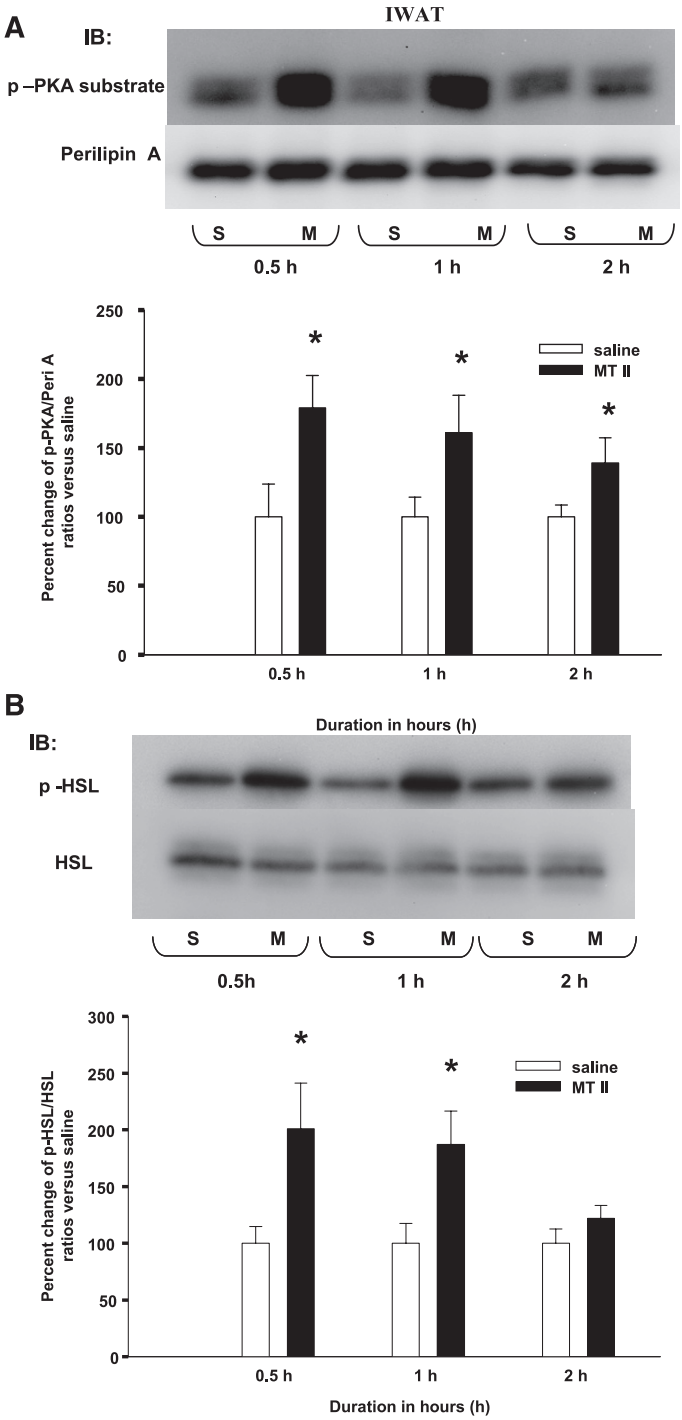

Fig. 3. *A*: mean ± SE ratios of IWAT p-Peri A as probed by the p-PKA Ser/Thr substrate antibody over the total Peri A as probed by Peril A antibody from hamsters given a single 3rd ventricle (3V) saline (S) or MTII (M) injection. The M group data are expressed as %change compared with the S group within each time period as represented in the bar graph. Samples were run in duplicates and the immunoblots (IB) were probed separately with either p-PKA Ser/Thr substrate (*top*) or Peri A (*bottom*) antibodies. $*P < 0.05$, MTII vs. S groups of the same time period. *B*: mean ± SE ratios of IWAT phosphorylated hormone-sensitive lipase (p-HSL) over the total HSL from hamsters given a single 3V MTII or saline injection. The M group data are expressed as % change compared with the S group within each time period. $*P < 0.05$, MTII vs. S groups of the same time period. Figure 3 is a composite of duplicate samples probed with different antibodies.

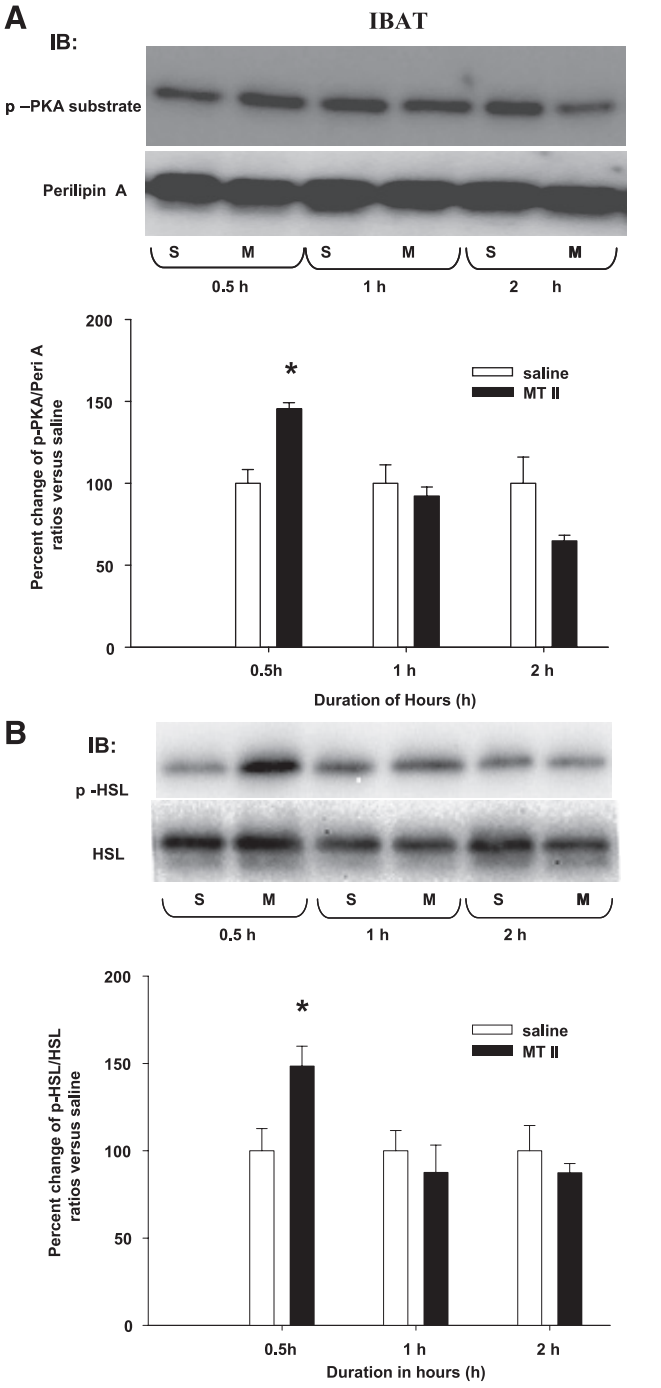

Fig. 4. *A*: mean ± SE ratios of interscapular brown adipose tissue (IBAT) p-Peri A as probed by the p-PKA Ser/Thr substrate antibody over the total Peri A as probed by Peri A antibody from hamsters given a single 3V saline (S) or MTII (M) injection. The M group data are expressed as %change compared with the S group within each time period as represented in the bar graph. Samples were run in duplicates and the immunoblots (IB) were probed separately with either p-PKA Ser/Thr substrate (*top*) or Peri A (*bottom*) antibodies. $*P < 0.05$, MTII vs. S groups of the same time period. *B*: mean ± SE ratios of IBAT p-HSL over the total HSL from hamsters given a single 3V MTII or saline injection. The M group data are expressed as % change compared with the S group within each time period. $*P < 0.05$, MTII vs. saline of the same time period. Figure 4 is a composite of duplicate samples probed with different antibodies.

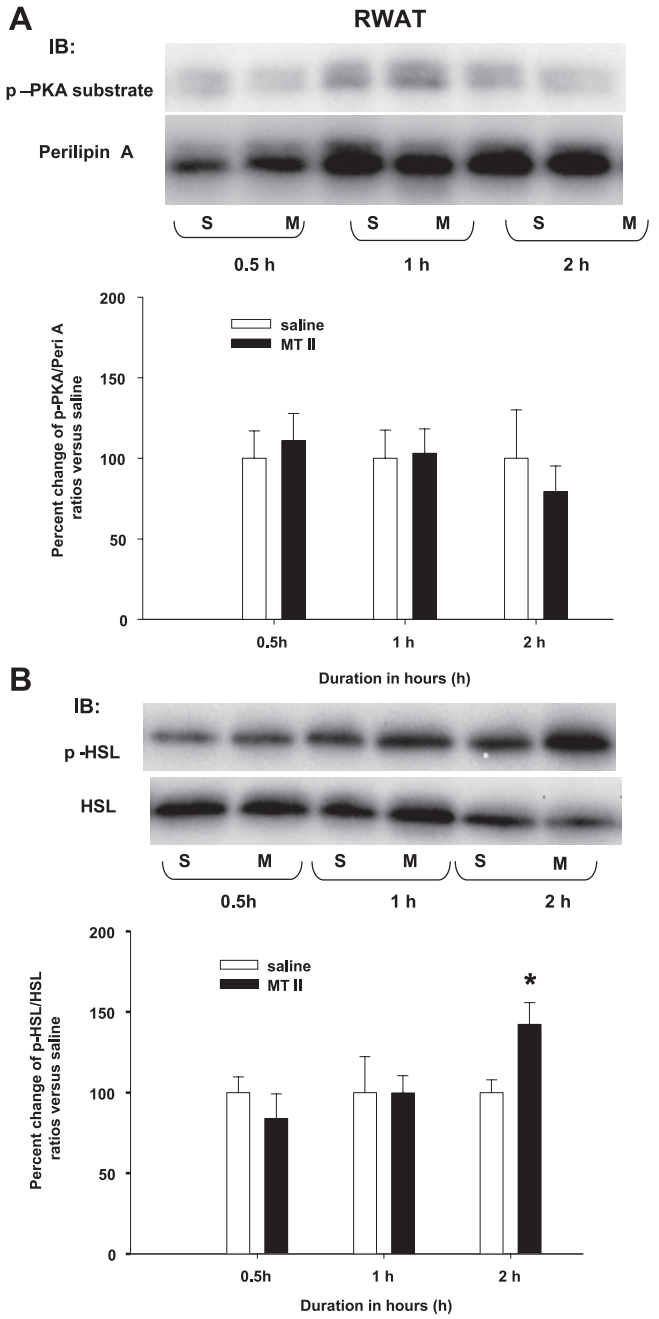

Fig. 5. *A*: mean ± SE ratios of retroperitoneal WAT (RWAT) p-Peri A as probed by the p-PKA Ser/Thr substrate antibody over the total Peri A as probed by Peri A antibody from hamsters given a single 3V saline (S) or MTII (M) injection. The M group data are expressed as %change compared with the S group within each time period as represented in the bar graph. Samples were run in duplicates and the immunoblots (IB) were probed separately with either p-PKA Ser/Thr substrate (*top*) or Peri A (*bottom*) antibodies. *B*: mean + SE ratios of RWAT p-HSL over the total HSL from hamsters given a single 3V MTII or saline injection. The M group data are expressed as %change compared with the S group within each time period. $*P < 0.05$, MTII vs. S groups of the same time period. Figure 5 is a composite of duplicate samples probed with different antibodies.

3V MTII administration triggered increased ratios of IBAT p-perilipin A to perilipin A and p-HSL to HSL compared with saline injected hamsters, but this effect was short lived only being significant at 30 min (compared with up to 120 min for IWAT in the present experiment). The exact reason for these time-truncated responses is unknown, but it could be due to the temporal sequence of intrabrown adipocyte signaling to the presumed MTII-induced increased sympathetic drive (NETO) to IBAT, seen previously with an identical treatment (14). That is, an initial response

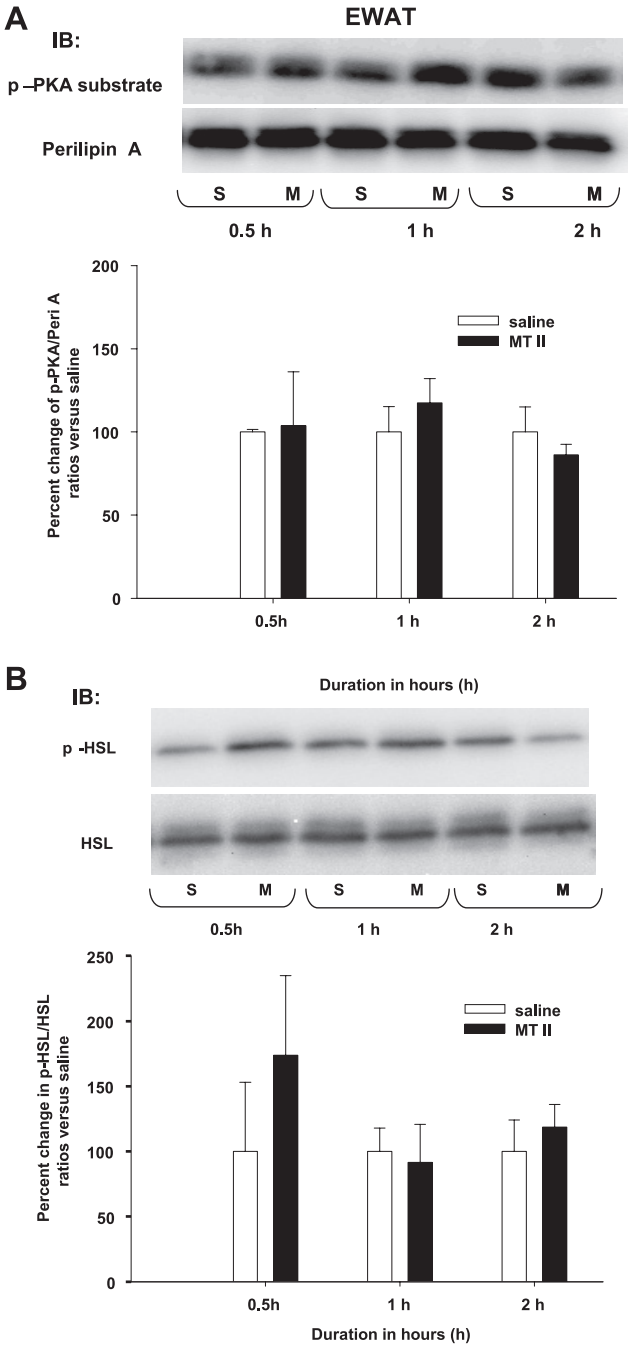

Fig. 6. *A*: mean ± SE ratios of epididymal WAT (EWAT) p-Peri A as probed by the p-PKA Ser/Thr substrate antibody over the total Peri A as probed by Peri A antibody from hamsters given a single 3V saline (S) or MTII (M) injection. The M group data are expressed as %change compared with the S group within each time period as represented in the bar graph. Samples were run in duplicates and the immunoblots (IB) were probed separately with either p-PKA Ser/Thr substrate (*top*) or Peri A (*bottom*) antibodies. *B*: mean + SE ratios of EWAT p-HSL over the total HSL from hamsters given a single 3V MTII or saline injection. The M group data are expressed as %change compared with the S group within each time period. Figure 6 is a composite of duplicate samples probed with different antibodies.

required for BAT thermogenesis is the phosphorylation of HSL and perilipin A and subsequent triacylglycerol hydrolysis (54), and this occurred 30 min postinjection here. It is believed that FFAs activate/reactivate UCP-1 in BAT mitochondria; thus, the need for triacylglycerol hydrolysis to increase BAT thermogenesis (50). Once activated, continued uncoupling appears to require FFAs competing against purine nucleotides for persisting activation. Therefore, if hydrolyzed FFAs are in ample supply from in situ triacylglycerols and/or are taken up via their mobilization from WAT due to melanocortin receptor agonism of the SNS drive to WAT (14), then the lack of subsequent increases in p-perilipin and p-HSL beyond the initial increase at 30 min may not be necessary. Indeed, when MTII is given centrally to Siberian hamsters identically to the treatment here (14), the increase in IBAT temperature first becomes significant at 60 min and lasting up to ~200 min postinjection, suggesting continued persistent uncoupling. Regardless, it is likely that this effect is mediated via central MC4-R via the SNS drive to IBAT in that 3V administration of a highly specific MC4-R agonist (cyclo[β-Ala-His-$_D$-Phe-Arg-Trp-Glu]NH_2) produces a similar, albeit smaller, increase in IBAT temperature in this species (14). Because of the general stimulation of periventricular hypothalamic, midbrain, and brain stem structures with 3V MTII, and because there are dozens of populations of neurons containing SNS outflow neurons to BAT possessing MC4-R mRNA (53), the exact sites responsible for the effects on BAT demonstrated here and previously (14) are unknown. One possible site, however, may be the hypothalamic paraventricular nucleus (PVN). The PVN has significant colocalization of SNS outflow neurons to IBAT possessing MC4-R mRNA [~80%; (53)]. Using an MTII dose below those able to trigger increases in IBAT temperature when injected into the 3V, acute parenchymal MTII microinjections into the PVN of awake, freely-moving Siberian hamsters, significantly increase IBAT temperature for as long as 4 h (53). Obviously this is only one of many other possible periventricular sites that would be exposed to MTII including those in the brain stem. In terms of the latter, we demonstrated that in chronically decerebrated laboratory rats receiving 4V MTII injections, IBAT UCP-1 gene expression is increased to the same extent as 3V MTII injections (60). Moreover, this effect is via the SNS innervation of IBAT because surgical denervation of the tissue blocks the increase in IBAT UCP1-mRNA (60).

In conclusion, the results from these experiments show that the increased circulating concentrations of the lipolytic products glycerol and FFAs (present study and Ref. 14) triggered by central melanocortin receptor agonism and resulting in differential increases in the sympathetic drive to WAT [increased IWAT, but not RWAT and EWAT (14)], likely derive from WAT pads that exhibited increased p-perilipin A and/or p-HSL IWAT, but not EWAT or RWAT. Therefore, increases in p-perilipin A and/or p-HSL can be used as indicators of fat pad-specific catecholamine-induced lipolysis in vivo. Our findings are concurrent with a recent report published during the preparation of the manuscript where there was a strong correlation between increases in p-perilipin A and stimulated lipolysis in vivo in WAT from the tail of lactating cows (27).

Perspectives and Significance

It is abundantly clear, even to the nonscientist, that the reversal of obesity is more effortful than the generation of the obese state. Our understanding of the processes that underlie reversals in adiposity have been aided by the relatively recent acknowledgement of the SNS innervation of WAT (3, 61) and that its activation is the principal initiator of lipolysis in mammals including, of course, humans (for reviews see Refs. 6, 8, and 9). In terms of the latter, there is recent evidence in humans that lipid mobilization during exercise may be an exception, with adrenal medullary epinephrine as the primary initiator of lipolysis (22), despite the unabated lipid mobilization that occurs to a variety of lipolytic stimuli in adrenal demedullated rodents (e.g., Refs. 44 and 59). In addition, atrial naturetic peptide is a powerful stimulator of lipolysis in human fat cells (34) that apparently is independent of SNS activation (28). Nevertheless, the elegant work of Dodt (23) demonstrates the importance of the sympathetic neural mechanism of lipolysis in humans. Specifically, intraneural electrical stimulation of the lateral femoral cutaneous nerve in vivo in humans leads to increases in lipolysis, as measured by recovery of glycerol from microdialysis probes in WAT innervated by this nerve (23). Indeed, further studies by Dodt (24) suggest less lipolysis occurs with this stimulation in obese humans vs. humans with normal adiposity levels, suggesting a possible role of sympathetic neural dysfunction in obesity. With the knowledge that catecholamine-stimulated lipolysis is nearly completely dependent on phosphorylation of HSL and perilipin A (for reviews see Refs. 12, 32, and 35), we capitalized on these findings to use p-HSL and p-perilipin A as in vivo, fat pad-specific intracellular markers of catecholamine (SNS)-stimulated lipolysis here. Using the identical lipolytic stimulus (central melanocortin receptor agonism by 3V injection of the same dose of MTII) that resulted in increases in the SNS drive (NETO) to some (IWAT and IBAT), but not all adipose tissue pads [EWAT and RWAT; (14)], here we found significant increases in the phosphorylation of perilipin A and HSL only in the depots where NETO was increased previously (IWAT, IBAT) but not in those that did have increases in NETO [EWAT and RWAT; (14)]. Therefore, this demonstration should permit the future use of this in vivo methodology to assay whether a given stimulus triggers SNS-induced lipolysis on a fat pad-specific basis, rather than having to rely on the presence of increases in circulating FFAs and/or glycerol of unknown origin. Given that the fat pads assayed by this methodology are tested for changes in phosphorylation of these proteins yield a snapshot in time of on-going processes, this will necessitate conducting time course studies to catch the lipolysis "in the act" of mobilizing lipid (i.e., in the process of phosphorylating perilipin A and HSL). This caveat aside, the ability to assess lipolysis on a fat pad-specific basis in vivo from as many adipose tissues as one desires, is a marked improvement from testing isolated fat cells from treated animals ex vivo after a treatment in the hopes that the effects of the lipolytic stimulus still lingers, or of microdialysis from one or two fat pads (most frequently accomplished in anesthetized animals; e.g., Ref. 46).

ACKNOWLEDGEMENTS

The authors thank Drs. Susan Fried, Dawn Brasaemle, and Andrew Greenberg for their helpful discussions and suggestions.

GRANTS

This work was supported, in part by National Institute of Diabetes and Digestive and Kidney Diseases Research Grant R37-DK-35254 (to T. J. Bartness).

DISCLOSURES

No conflicts of interest, financial or otherwise, are declared by the author(s).

REFERENCES

1. **Anthonsen MW, Ronnstrand L, Wernstedt C, Degerman E, Holm C.** Identification of novel phosphorylation sites in hormone-sensitive lipase that are phosphorylated in response to isoproterenol and govern activation properties in vitro. *J Biol Chem* 273: 215–221, 1998.
2. **Arner P.** Human fat cell lipolysis: biochemistry, regulation and clinical role. *Best Pract Res Clin Endocrinol Metab* 19: 471–482, 2005.
3. **Bamshad M, Aoki VT, Adkison MG, Warren WS, Bartness TJ.** Central nervous system origins of the sympathetic nervous system outflow to white adipose tissue. *Am J Physiol Regul Integr Comp Physiol* 275: R291–R299, 1998.
4. **Bamshad M, Song CK, Bartness TJ.** CNS origins of the sympathetic nervous system outflow to brown adipose tissue. *Am J Physiol Regul Integr Comp Physiol* 276: R1569–R1578, 1999.
5. **Baro DJ, Levini RM, Kim MT, Willms AR, Lanning CC, Rodriguez HE, Harris-Warrick RM.** Quantitative single-cell-reverse transcription-PCR demonstrates that A-current magnitude varies as a linear function of *shal* gene expression in identified stomatogastric neurons. *J Neurosci* 17: 6597–6610, 1997.
6. **Bartness TJ, Bamshad M.** Innervation of mammalian white adipose tissue: implications for the regulation of total body fat. *Am J Physiol Regul Integr Comp Physiol* 275: R1399–R1411, 1998.
7. **Bartness TJ, Morley JE, Levine AS.** Photoperiod-peptide interactions in the energy intake of Siberian hamsters. *Peptides* 7: 1079–1085, 1986.
8. **Bartness TJ, Song CK.** Sympathetic and sensory innervation of white adipose tissue. *J Lipid Res* 48: 1655–1672, 2007.
9. **Bartness TJ, Song CK, Shi H, Bowers RR, Foster MT.** Brain-adipose tissue cross talk. *Proc Nutr Soc* 64: 53–64, 2005.
10. **Boston BA, Cone RD.** Characterization of melanocortin receptor subtype expression in murine adipose tissues and in the 3T3–L1 cell line. *Endocrinology* 137: 2043–2050, 1996.
11. **Bradley RL, Mansfield JP, Maratos-Flier E.** Neuropeptides, including neuropeptide Y and melanocortins, mediate lipolysis in murine adipocytes. *Obes Res* 13: 653–661, 2005.
12. **Brasaemle DL.** The perilipin family of structural lipid droplet proteins: stabilization of lipid droplets and control of lipolysis. *J Lipid Res* 48: 2547–2559, 2007.
13. **Brasaemle DL, Rubin B, Harten IA, Gruia-Gray J, Kimmel AR, Londos C.** Perilipin A increases triacylglycerol storage by decreasing the rate of triacylglycerol hydrolysis. *J Biol Chem* 275: 38486–38493, 2000.
14. **Brito MN, Brito NA, Baro DJ, Song CK, Bartness TJ.** Differential activation of the sympathetic innervation of adipose tissues by melanocortin receptor stimulation. *Endocrinology* 148: 5339–53347, 2007.
15. **Brito NA, Brito MN, Bartness TJ.** Differential sympathetic drive to adipose tissues after food deprivation, cold exposure or glucoprivation. *Am J Physiol Regul Integr Comp Physiol* 294: R1445–R1452, 2008.
16. **Butler AA.** The melanocortin system and energy balance. *Peptides* 27: 281–290, 2006.
17. **Carmen GY, Victor SM.** Signalling mechanisms regulating lipolysis. *Cell Signal* 18: 401–408, 2006.
18. **Clifford GM, McCormick DK, Londos C, Vernon RG, Yeaman SJ.** Dephosphorylation of perilipin by protein phosphatases present in rat adipocytes. *FEBS Lett* 435: 125–129, 1998.
19. **Cohen AW, Razani B, Schubert W, Williams TM, Wang XB, Iyengar P, Brasaemle DL, Scherer PE, Lisanti MP.** Role of caveolin-1 in the modulation of lipolysis and lipid droplet formation. *Diabetes* 53: 1261–1270, 2004.
20. **Collins S, Migliorini RH, Bartness TJ.** Mechanisms controlling adipose tissue metabolism by the sympathetic nervous system: anatomical and molecular aspects. In: *Handbook of Contemporary Neuropharmacology*, edited by Sibley D, Hanin I, Kuhar M, and Skolnick P. New York: Wiley, 2007, p. 785–814.
21. **Day DE, Bartness TJ.** Agouti-related protein increases food hoarding, but not food intake by Siberian hamsters. *Am J Physiol Regul Integr Comp Physiol* 286: R38–R45, 2004.
22. **de Glisezinski I, Larrouy D, Bajzova M, Koppo K, Polak J, Berlan M, Bolow J, Langin D, Marques MA, Crampes F, Lafontan M, Stich V.** Adrenaline but not noradrenaline is a determinant of exercise-induced lipid mobilization in human subcutaneous adipose tissue. *J Physiol* 587: 3393–3404, 2009.
23. **Dodt C, Lonnroth P, Fehm HL, Elam M.** Intraneural stimulation elicits an increase in subcutaneous interstitial glycerol levels in humans. *J Physiol* 521: 545–552, 1999.
24. **Dodt C, Lonnroth P, Wellhoner JP, Fehm HL, Elam M.** Sympathetic control of white adipose tissue in lean and obese humans. *Acta Physiol Scand* 177: 351–357, 2003.
25. **Egan JJ, Greenberg AS, Chang MK, Londos C.** Control of endogenous phosphorylation of the major cAMP-dependent protein kinase substrate in adipocytes by insulin and β-adrenergic stimulation. *J Biol Chem* 265: 18769–18775, 1990.
26. **Egan JJ, Greenberg AS, Chang MK, Wek SA, Moos MC Jr, Londos C.** Mechanism of hormone-stimulated lipolysis in adipocytes: translocation of hormone-sensitive lipase to the lipid storage droplet. *Proc Natl Acad Sci USA* 89: 8537–8541, 1992.
27. **Elkins DA, Spurlock DM.** Phosphorylation of perilipin is associated with indicators of lipolysis in Holstein cows. *Horm Metab Res* 2009.
28. **Galitzky J, Sengenes C, Thalamas C, Marques MA, Senard JM, Lafontan M, Berlan M.** The lipid-mobilizing effect of atrial natriuretic peptide is unrelated to sympathetic nervous system activation or obesity in young men. *J Lipid Res* 42: 536–544, 2001.
29. **Greenberg AS, Egan JJ, Wek SA, Garty NB, Blanchette-Mackie EJ, Londos C.** Perilipin, a major hormonally regulated adipocyte-specific phosphoprotein associated with the periphery of lipid storage droplets. *J Biol Chem* 266: 11341–11346, 1991.
30. **Greenberg AS, Egan JJ, Wek SA, Moos MC Jr, Londos C, Kimmel AR.** Isolation of cDNAs for perilipins A and B: sequence and expression of lipid droplet-associated proteins of adipocytes. *Proc Natl Acad Sci USA* 90: 12035–12039, 1993.
31. **Hoggard N, Hunter L, Duncan JS, Rayner DV.** Regulation of adipose tissue leptin secretion by α-melanocyte-stimulating hormone and agouti-related protein: further evidence of an interaction between leptin and the melanocortin signalling system. *J Mol Endocrinol* 32: 145–153, 2004.
32. **Holm C.** Molecular mechanisms regulating hormone-sensitive lipase and lipolysis. *Biochem Soc Trans* 31: 1120–1124, 2003.
33. **Lafontan M, Bousquet-Melou A, Galitzky J, Barbe P, Carpene C, Langin D, Valet P, Castan I, Bouloumie A, Saulnier-Blache JS.** Adrenergic receptors and fat cells: differential recruitment by physiological amines and homologous regulation. *Obes Res* 3: 507S–514S, 1995.
34. **Lafontan M, Sengenes C, Galitzky J, Berlan M, de Glisezinski I, Crampes F, Stich V, Langin D, Barbe P, Riviere D.** Recent developments on lipolysis regulation in humans and discovery of a new lipolytic pathway. *Int J Obes Relat Metab Disord* 24, *Suppl 4*: S47–S52, 2000.
35. **Langin D.** Adipose tissue lipolysis as a metabolic pathway to define pharmacological strategies against obesity and the metabolic syndrome. *Pharmacol Res* 53: 482–491, 2006.
36. **Langin D, Dicker A, Tavernier G, Hoffstedt J, Mairal A, Ryden M, Arner E, Sicard A, Jenkins CM, Viguerie N, van H, V, Gross RW, Holm C, Arner P.** Adipocyte lipases and defect of lipolysis in human obesity. *Diabetes* 54: 3190–3197, 2005.
37. **Londos C, Brasaemle DL, Schultz CJ, Adler-Wailes DC, Levin DM, Kimmel AR, Rondinone CM.** On the control of lipolysis in adipocytes. *Ann NY Acad Sci* 892: 155–168, 1999.
38. **Lonnqvist F, Thome A, Nilsell K, Hoffstedt J, Arner P.** A pathogenic role of visceral fat β_3-adrenoceptors in obesity. *J Clin Invest* 95: 1109–1116, 1995.
39. **Marcinkiewicz A, Gauthier D, Garcia A, Brasaemle DL.** The phosphorylation of serine 492 of perilipin A directs lipid droplet fragmentation and dispersion. *J Biol Chem* 281: 11901–11909, 2006.
40. **Martinez-Botas J, Anderson JB, Tessier D, Lapillonne A, Chang BH, Quast MJ, Gorenstein D, Chen KH, Chan L.** Absence of perilipin results in leanness and reverses obesity in *Lepr*(*db/db*) mice. *Nat Genet* 26: 474–479, 2000.
41. **Miyoshi H, Souza SC, Zhang HH, Strissel KJ, Christoffolete MA, Kovsan J, Rudich A, Kraemer FB, Bianco AC, Obin MS, Greenberg**

AS. Perilipin promotes hormone-sensitive lipase-mediated adipocyte lipolysis via phosphorylation-dependent and -independent mechanisms. *J Biol Chem* 281: 15837–15844, 2006.
42. **Moore HP, Silver RB, Mottillo EP, Bernlohr DA, Granneman JG.** Perilipin targets a novel pool of lipid droplets for lipolytic attack by hormone-sensitive lipase. *J Biol Chem* 280: 43109–43120, 2005.
43. **Newsholme EA, Leech AR.** *Biochemistry for the Medical Sciences*. Chichester, UK: Wiley, 1983.
44. **Nishizawa Y, Bray GA.** Ventromedial hypothalamic lesions and the mobilization of fatty acids. *J Clin Invest* 61: 714–721, 1978.
45. **Nogueiras R, Wiedmer P, Perez-Tilve D, Veyrat-Durebex C, Keogh JM, Sutton GM, Pfluger PT, Castaneda TR, Neschen S, Hofmann SM, Howles PN, Morgan DA, Benoit SC, Szanto I, Schrott B, Schurmann A, Joost HG, Hammond C, Hui DY, Woods SC, Rahmouni K, Butler AA, Farooqi IS, O'Rahilly S, Rohner-Jeanrenaud F, Tschop MH.** The central melanocortin system directly controls peripheral lipid metabolism. *J Clin Invest* 117: 3475–3488, 2007.
46. **Portillo MP, Villaro JM, Torres MI, Macarulla MT.** In vivo lipolysis in adipose tissue from two anatomical locations measured by microdialysis. *Life Sci* 67: 437–445, 2000.
47. **Raposinho PD, White RB, Aubert ML.** The melanocortin agonist melanotan-II reduces the orexigenic and adipogenic effects of neuropeptide Y (NPY) but does not affect the NPY-driven suppressive effects on the gonadotropic and somatotropic axes in the male rat. *J Neuroendocrinol* 15: 173–181, 2003.
48. **Ryden M, Jocken J, van H, V, Dicker A, Hoffstedt J, Wiren M, Blomqvist L, Mairal A, Langin D, Blaak E, Arner P.** Comparative studies of the role of hormone-sensitive lipase and adipose triglyceride lipase in human fat cell lipolysis. *Am J Physiol Endocrinol Metab* 292: E1847–E1855, 2007.
49. **Schioth HB, Lagerstrom MC, Watanobe H, Jonsson L, Vergoni AV, Ringholm A, Skarphedinsson JO, Skuladottir GV, Klovins J, Fredriksson R.** Functional role, structure, and evolution of the melanocortin-4 receptor. *Ann NY Acad Sci* 994: 74–83, 2003.
50. **Shabalina IG, Jacobsson A, Cannon B, Nedergaard J.** Native UCP1 displays simple competitive kinetics between the regulators purine nucleotides and fatty acids. *J Biol Chem* 279: 38236–38248, 2004.
51. **Soeder KJ, Snedden SK, Cao W, Della Rocca GJ, Daniel KW, Luttrell LM, Collins S.** The β_3-adrenergic receptor activates mitogen-activated protein kinase in adipocytes through a G_i-dependent mechanism. *J Biol Chem* 274: 12017–12022, 1999.
52. **Song CK, Jackson RM, Harris RB, Richard D, Bartness TJ.** Melanocortin-4 receptor mRNA is expressed in sympathetic nervous system outflow neurons to white adipose tissue. *Am J Physiol Regul Integr Comp Physiol* 289: R1467–R1476, 2005.
53. **Song CK, Vaughan CH, Keen-Rhinehart E, Harris RB, Richard D, Bartness TJ.** Melanocortin-4 receptor mRNA expressed in sympathetic outflow neurons to brown adipose tissue: neuroanatomical and functional evidence. *Am J Physiol Regul Integr Comp Physiol* 295: R417–R428, 2008.
54. **Souza SC, Christoffolete MA, Ribeiro MO, Miyoshi H, Strissel KJ, Stancheva ZS, Rogers NH, D'Eon TM, Perfield JW, Imachi H, Obin MS, Bianco AC, Greenberg AS.** Perilipin regulates the thermogenic actions of norepinephrine in brown adipose tissue. *J Lipid Res* 48: 1273–1279, 2007.
55. **Souza SC, de Vargas LM, Yamamoto MT, Lien P, Franciosa MD, Moss LG, Greenberg AS.** Overexpression of perilipin A and B blocks the ability of tumor necrosis factor-α to increase lipolysis in 3T3–L1 adipocytes. *J Biol Chem* 273: 24665–24669, 1998.
56. **Sztalryd C, Xu G, Dorward H, Tansey JT, Contreras JA, Kimmel AR, Londos C.** Perilipin A is essential for the translocation of hormone-sensitive lipase during lipolytic activation. *J Cell Biol* 161: 1093–1103, 2003.
57. **Tansey JT, Huml AM, Vogt R, Davis KE, Jones JM, Fraser KA, Brasaemle DL, Kimmel AR, Londos C.** Functional studies on native and mutated forms of perilipins. A role in protein kinase A-mediated lipolysis of triacylglycerols. *J Biol Chem* 278: 8401–8406, 2003.
58. **Tansey JT, Sztalryd C, Gruia-Gray J, Roush DL, Zee JV, Gavrilova O, Reitman ML, Deng CX, Li C, Kimmel AR, Londos C.** Perilipin ablation results in a lean mouse with aberrant adipocyte lipolysis, enhanced leptin production, and resistance to diet-induced obesity. *Proc Natl Acad Sci USA* 98: 6494–6499, 2001.
59. **Teixeira VL, Antunes-Rodrigues J, Migliorini RH.** Evidence for centers in the central nervous system that selectively regulate fat mobilization in the rat. *J Lipid Res* 14: 672–677, 1973.
60. **Williams DL, Bowers RR, Bartness TJ, Kaplan JM, Grill HJ.** Brainstem melanocortin 3/4 receptor stimulation increases uncoupling protein gene expression in brown fat. *Endocrinology* 144: 4692–4697, 2003.
61. **Youngstrom TG, Bartness TJ.** Catecholaminergic innervation of white adipose tissue in the Siberian hamster. *Am J Physiol Regul Integr Comp Physiol* 268: R744–R751, 1995.
62. **Zu L, Jiang H, He J, Xu C, Pu S, Liu M, Xu G.** Salicylate blocks lipolytic actions of tumor necrosis factor-α in primary rat adipocytes. *Mol Pharmacol* 73: 215–223, 2008.